IVYSPRING INTERNATIONAL PUBLISHER

Theranostics

2018; 8(3): 710-722. doi: 10.7150/thno.19154

Research Paper

General Anesthesia Inhibits the Activity of the "Glymphatic System"

Clement Gakuba[1, 2]✉, Thomas Gaberel[1, 3], Suzanne Goursaud[1, 2], Jennifer Bourges[1, 2], Camille Di Palma[1, 3], Aurélien Quenault[1], Sara Martinez de Lizarrondo[1], Denis Vivien[1, 4], Maxime Gauberti[1, 5]✉

1. Normandie Univ, UNICAEN, INSERM, INSERM UMR-S U1237, "Physiopathology and Imaging of Neurological Disorders" PhIND, 14000 Caen, France;
2. CHU Caen, Department of Anesthesiology and Critical Care Medicine, CHU Caen Côte de Nacre, 14000 Caen, France;
3. CHU Caen, Department of Neurosurgery, CHU Caen Côte de Nacre, 14000 Caen, France;
4. CHU Caen, Department of Cell Biology, CHU Caen Côte de Nacre, 14000 Caen, France;
5. CHU Caen, Department of Diagnostic Imaging and Interventional Radiology, CHU Caen Côte de Nacre, 14000 Caen, France.

✉ Corresponding authors: Maxime GAUBERTI (gauberti@cyceron.fr) or Clement GAKUBA (gakuba@cyceron.fr), INSERM, UMR-S U1237, "Physiopathology and Imaging of Neurological Disorders" PhIND, GIP Cyceron, Caen-Normandy University, Bd Henri Becquerel, Caen, France. Phone: +33.2.31.47.01.66, Fax: +33.2.31.47.02.22.

Received: 2017.01.12; Accepted: 2017.10.21; Published: 2018.01.01

Abstract

INTRODUCTION: According to the "glymphatic system" hypothesis, brain waste clearance is mediated by a continuous replacement of the interstitial milieu by a bulk flow of cerebrospinal fluid (CSF). Previous reports suggested that this cerebral CSF circulation is only active during general anesthesia or sleep, an effect mediated by the dilatation of the extracellular space. Given the controversies regarding the plausibility of this phenomenon and the limitations of currently available methods to image the glymphatic system, we developed original whole-brain *in vivo* imaging methods to investigate the effects of general anesthesia on the brain CSF circulation.

METHODS: We used magnetic resonance imaging (MRI) and near-infrared fluorescence imaging (NIRF) after injection of a paramagnetic contrast agent or a fluorescent dye in the cisterna magna, in order to investigate the impact of general anesthesia (isoflurane, ketamine or ketamine/xylazine) on the intracranial CSF circulation in mice.

RESULTS: *In vivo* imaging allowed us to image CSF flow in awake and anesthetized mice and confirmed the existence of a brain-wide CSF circulation. Contrary to what was initially thought, we demonstrated that the parenchymal CSF circulation is mainly active during wakefulness and significantly impaired during general anesthesia. This effect was especially significant when high doses of anesthetic agent were used (3% isoflurane). These results were consistent across the different anesthesia regimens and imaging modalities. Moreover, we failed to detect a significant change in the brain extracellular water volume using diffusion weighted imaging in awake and anesthetized mice.

CONCLUSION: The parenchymal diffusion of small molecular weight compounds from the CSF is active during wakefulness. General anesthesia has a negative impact on the intracranial CSF circulation, especially when using a high dose of anesthetic agent.

Key words: glymphatic system, anesthesia, magnetic resonance imaging, Alzheimer, choroid plexus.

Introduction

The classical textbook model of cerebrospinal fluid (CSF) circulation in the brain describes a CSF production by the choroid plexus, followed by its flow through the ventricles and the subarachnoid spaces, finally exiting from the brain through the arachnoid granulations. Based on earlier work from Cserr [1-3], Weller [4] and others, recent studies suggest that the physiology of CSF circulation may be more complicated than initially thought [5-7]. In this context, the description of the glymphatic system by the group of M. Nedergaard has challenged our understanding of CSF circulation by describing a bulk

flow of CSF between arterial and venous paravascular spaces in the brain parenchyma [8, 9]. This system was reported to drive the cleaning of the brain from accumulated metabolites, such as the beta-amyloid peptide, through a convective flow of CSF in the brain parenchyma following a para-arterial entry route and a para-venular efflux [10]. Therefore, some evidence suggests that the glymphatic system plays a key role in the pathophysiology of neurodegenerative disorders [11], including recent results in patients with Alzheimer's disease [12]. The interest in this system was further amplified with the recent description of functional lymphatic vessels along cerebral venous sinuses in the adult brain [13, 14].

Previous studies suggested that the glymphatic system was only active during sleep or general anesthesia, an effect mediated by an increase of 60% of the brain extracellular volume [15]. However, general anesthesia has been associated with beta-amyloid peptide aggregation and tau hyperphosphorilation in preclinical studies [16]. In humans, observational clinical studies revealed that cerebrospinal fluid biomarkers convert to an Alzheimer's disease pattern after general anesthesia [17, 18]. Additionally, discordant results on brain waste clearance under anesthesia are reported in the literature [15, 19], in particular regarding the role of CSF mediated clearance [20]. Indeed, due to technical limitations, most previous studies failed to investigate CSF circulation dynamics in the whole brain using non-invasive methods, but instead relied on superficial measurement (~100 µm beneath the cortical surface) of tracer diffusion in the brain of craniotomized mice, thus potentially leading to misrepresentation of the whole CSF circulation. Moreover, the glymphatic concept and the expansion of the extracellular volume during general anesthesia have been challenged by several recent studies [20-23]. In this context, the impact of general anesthesia on the parenchymal CSF flow remains elusive.

Here, we developed original approaches allowing whole brain imaging of the CSF circulation in awake and anesthetized mice using contrast-enhanced magnetic resonance imaging (MRI), near-infrared fluorescence (NIRF) and diffusion-weighted imaging. We present results demonstrating that the parenchymal diffusion of low molecular weight compounds administered in the CSF is reduced in anesthetized mice when compared with awake animals, therefore suggesting that general anesthesia impairs the circulation of CSF through the brain.

Methods

Approval

Animal experiments were approved by the local ethical committee (C-31.555-07, US006 CREFRE (CEEA-122)) and were performed in accordance with the French (Decree 87/848) and the European Communities Council (Directive 2010/63/EU) guidelines.

Animals and anesthesia

Experiments were performed in male Swiss mice (35-40g; CURB, Caen, France) housed with a 12 h light/12 h dark cycle. All the experiments were performed at the same time of the dark phase corresponding to mice waking hours (8-10 PM). Surgical procedures were performed under 2% isoflurane. Thereafter, mice were ether allowed to recover or maintained under general anesthesia for a 30 min or 60 min period: isoflurane (2-2.5% except if indicated otherwise), ketamine (150 mg/kg, intraperitoneal) or ketamine/xylazine (100 mg/kg ketamine and 10 mg/kg xylazine). When anesthetized, mouse body temperature was monitored and maintained at 37°C with a rectal temperature probe and homeothermic heating pad. Hypnosis for mice placed under general anesthesia was established by control of loss of righting reflex, absence of limb withdrawal when applying pressure to the paw and monitoring of mean arterial pressure, and heart and respiratory rates. Awakening of the mice after purging volatile anesthetic from the ventilation system during MRI experiments was assessed by paraclinical (plethysmography) and clinical observation (responses to tactile stimulations). Mice were in prone position both in the awake and anesthesia conditions [24].

Intracisternal injection

Intracisternal injection was performed as previously described [25]. Briefly, a glass micropipette was inserted in the cisterna magna of anesthetized mice (isoflurane, 2-2.5%). Then, 1 µL or 3 µL of contrast agent was injected over 1 min (either gadolinium chelates, Evan's blue or indocyanine green). At the end of the injection, the pipette was left in place for 1 additional minute to prevent reflow. Then the surgical site was closed after thorough control under microscope view of the absence of any fluid leakage from the cisterna magna and the mice were awakened. The injection procedure took <5 min per animal (allowing a short anesthesia duration).

Contrast enhanced MRI

After injection of 1-3 µL of DOTA-Gd

(DOTAREM®, Guerbet, France) in the cisterna magna, the mice were either allowed to recover or maintained under anesthesia. MRI was performed 60 min thereafter on a 7T Pharmascan MRI system (Bruker, Germany) equipped with volume transmit and surface receive coils [26]. High-resolution 3D T_1-weighted imaging was performed with a Fast Low Angle Shot (FLASH) sequence with parameters set as follow: TR/TE 15/3.57 ms, Angle = 25°, Field of View = 20 × 17 × 14.4 mm, Matrix = 256 × 218 × 96 leading to a resolution of 78 × 78 × 0.15 µm, acquisition time = 5 min 14 s. Quantification of the images was performed using ImageJ (1.48, NIH) in a blinded manner and regions of interest were set in the brain regions described in Figure 1. The signal intensity ratio was computed by dividing the signal intensity in the region of interest by an arbitrarily selected region without DOTA-Gd (vitreous humor of the right eye, Figure S1).

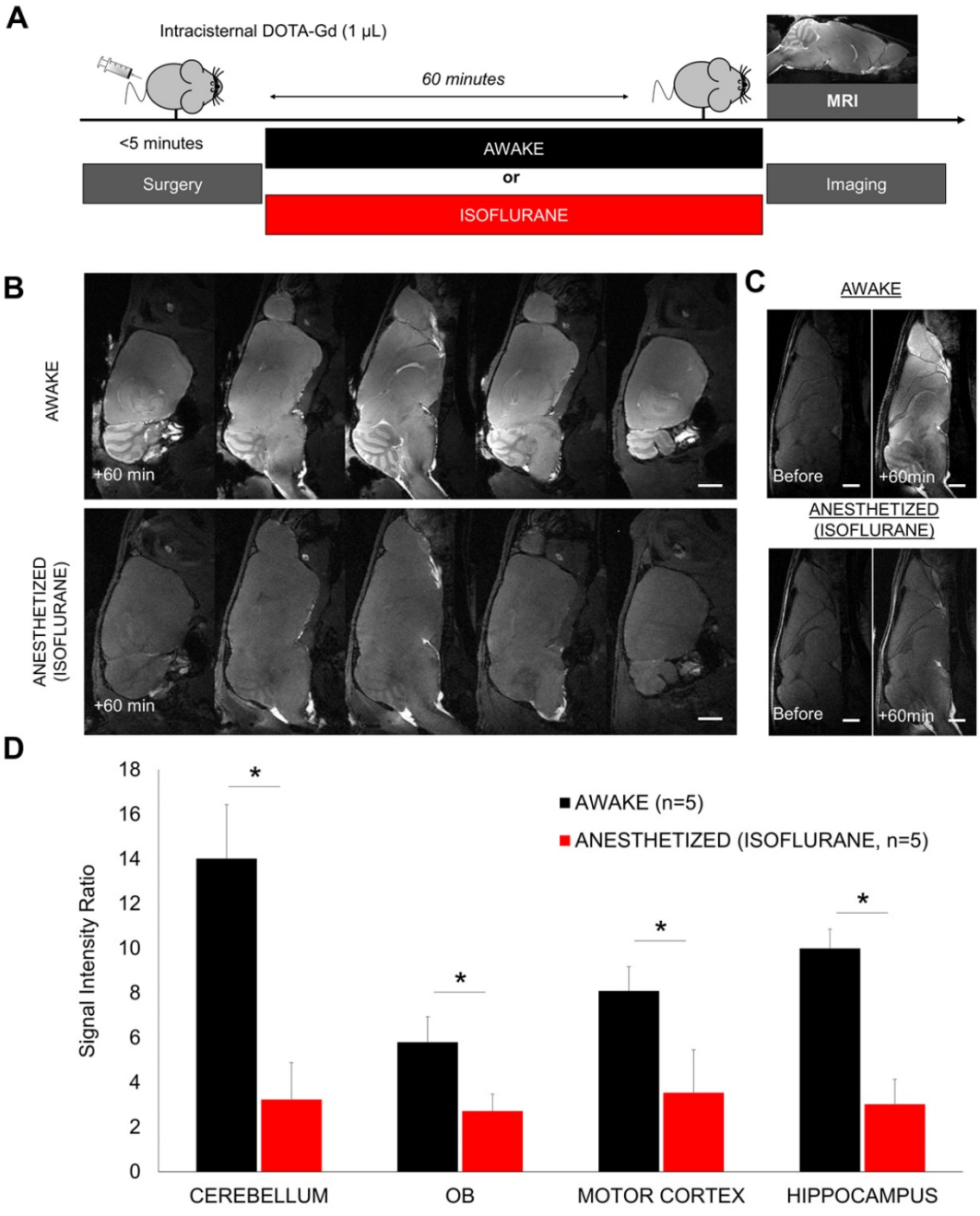

Figure 1. Gadolinium-enhanced magnetic resonance imaging of the brain after intracisternal injection of DOTA-Gd followed by wakefulness or isoflurane general anesthesia. (A) Schematic representation of the experimental design of the Magnetic Resonance Imaging (MRI) experiments. **(B)** Representative high-resolution T1-weighted images 60 min after intracisternal injection of DOTA-Gd (1 µL) in awake (top) and anesthetized mice (isoflurane 2-2.5%, bottom). Whereas DOTA-Gd (materialized by an increased signal intensity) was present mainly in the cerebrospinal fluid (CSF) of anesthetized mice, it was found in the whole brain of awake animals. **(C)** Representative high-resolution T_1-weighted images before and 60 min after intracisternal injection of DOTA-Gd (1 µL) in awake (top) and anesthetized mice (bottom). **(D)** Corresponding quantification of the signal intensity in four different regions of interest (Cerebellum, Olfactory Bulbs (OB), Motor Cortex and Hippocampus). The signal intensity ratio is significantly more important in the awake group, supporting an increased activity of the CSF circulation during wakefulness when compared to anesthetized animals (n=5 mice per group). Scale bar: 2 mm.

Ex vivo NIRF imaging

After injection of 1 µL of Evans Blue (4%, in phosphate buffered saline, Sigma) in the cisterna magna, the mice were either allowed to recover from anesthesia or maintained under isoflurane (2%) or ketamine (150 mg/kg, intraperitoneal). 30 min thereafter, the mice were euthanatized by overdose of isoflurane and the brain was removed to perform *ex vivo* NIRF imaging. The brain was placed in a photon-imager (Biospace, France) and images were acquired with excitation filter set at 600 nm and emission filter at 700 nm. The region of interest used for quantitative fluorometry encompassed the whole forebrain for the dorsal part, and the whole brain for the ventral part.

In vivo NIRF imaging of the glymphatic system

After injection of 1 µL of indocyanine green (ICG, 10 mg/mL, in phosphate buffered saline, Sigma-Aldrich) in the cisterna magna, the mice were either allowed to recover from anesthesia or maintained under isoflurane (2%). The mice were thereafter placed in a photon-imager for 60 min and real time imaging (22 ms per frame) was performed with excitation filter set at 650 nm and emission filter at 770 nm. Quantification was performed using the built-in software of the photon-imager in the forebrain, at distance from the injection site (cisterna magna). The background value was defined on the pre-injection image for each region (especially the forebrain) and then the photon count measured on each time-point was divided by this value to get the normalized photon count. The "+5 min" image was used to define the "cisterna magna" region, allowing us to define the anterior part of the head as the forebrain.

ADC measurement by MRI

Mice were accustomed to staying awake in the MRI animal holder for 3 weeks. The day of the experiment, the mice were placed under anesthesia (2% isoflurane) in the magnet to allow the first measurement of the ADC. Diffusion-weighted imaging data were collected by using an echo-planar sequence with two b factors (0 and 1000 s/mm^2) in 6 gradient directions with the following acquisition parameters: TR/TE 2500/40 ms; Matrix = 96 × 96, acquisition time = 10 s. A total of 10, 1 mm thick sections (0.5 mm gap) were acquired to cover the entire brain. ADC maps were computed using a homemade macro in ImageJ [27]. Briefly, the ADC was computed using 3 diffusion-weighted acquisitions (along 3 orthogonal diffusion directions) and a control, non-diffusion weighted acquisition. In this condition, calculation of the ADC is performed in each direction (x, y and z) using the following equation: $ADC(x, y, z) = \ln [S_2(x,y,z) / S_1 (x, y, z)] / (b_1 - b_2)$. We then computed the mean ADC as the arithmetic mean of ADCx, ADCy and ADCz using b values of 0 s/mm^2 and 1000 s/mm^2.

Physiological monitoring

Physiological data on temperature, blood pressure, heart rate and respiratory rate were acquired on separate groups of mice. Since the collection of these data required an invasive monitor installed under general anesthesia, we choose to perform these measures on other sets of mice to avoid prolonged general anesthesia when exploring the influence of anesthetics on CSF dynamics. Cannulation of the right femoral artery was performed with a polyethylene catheter connected to a pressure transducer coupled to a data acquisition system allowing continuous arterial pressure and heart rate monitoring. Ventilatory function was evaluated by plethysmography. During MRI, the temperature was maintained using temperature controlled warming blanket (Brüker). During NIRF imaging, the temperature was controlled using rectal probes and regulated manually using the built-in heating system (Biospace).

Actimetry

Spontaneous locomotor activity (horizontal and vertical movements) was quantified over 60 min using actimetry cages (Imetronic, Pessac, France). Measurements were performed immediately after a 5 min period of 2% isoflurane anesthesia or a sham manipulation of the mice.

Statistics

Results are the mean ± SD. When comparing two groups, statistical analyses were performed using the Mann-Whitney *U* test. When comparing more than two groups, statistical analyses were performed using the Kruskall-Wallis test followed by post hoc comparison with the Mann-Whitney *U* test. When analyzing longitudinal values (*in vivo* NIRF), we considered each time point as an independent measurement and compared the two groups using the Mann-Whitney U test.

Results

General anesthesia reduces the diffusion of intracisternally administered DOTA-Gd in the brain parenchyma.

We first evaluated the brain distribution of a low molecular weight compound (DOTA-Gd) after injection in the cisterna magna in anesthetized (2-2.5% of isoflurane) or awake mice (Figure 1A-B). DOTA-Gd

distribution was revealed 60 min after injection using MRI of the whole brain. MRI confirmed that DOTA-Gd penetrates the brain parenchyma using the glymphatic pathways as previously reported [25, 28]. But surprisingly, the concentration of DOTA-Gd was significantly higher in the awake mice in comparison with the isoflurane anesthetized mice in all the brain regions examined (Figure 1B-D). These data suggested that the CSF inflow is more active in awake mice.

An alternative interpretation of these findings could be that tracers were cleared more rapidly under anesthesia; thus, when imaging of the brains was performed 60 min post tracer injection, lower concentration of DOTA-Gd could be detected in the brain parenchyma of anesthetized versus awake animals. To address this potential issue, we first performed sequential imaging of mice placed under isoflurane anesthesia with high-resolution T_1-weighted images acquired every 5 min after intracisternal injection of DOTA-Gd (Figure 2A-B). We confirmed that maximal enhancement of brain parenchyma does not occur before 60 min under isoflurane anesthesia, ruling out the possibility of an accelerated clearance of DOTA-Gd. Moreover, in a similar experiment with an earlier 30 min endpoint, the concentration of DOTA-Gd was significantly higher in the awake mice in comparison with the isoflurane anesthetized mice in the olfactory bulbs, without significant difference in the other tested brain regions (Figure S2).

However, if not through the brain, where does the CSF in anesthetized mice go? To address this question, we performed sequential imaging of mice placed under isoflurane anesthesia after intracisternal injection of a higher dose (3 µL) of DOTA-Gd to increase the sensitivity of detection of CSF distribution. This higher dose allowed us to detect the CSF exit routes outside the brain. As shown on Figure 2C, we observed a slow diffusion of DOTA-Gd in the brain parenchyma in close vicinity to the ventral basal cisterns. Of note, the cerebellum remained free of detectable DOTA-Gd after 60 min, which is in sharp contrast with what was observed in awake mice (Figure 2D). Longitudinal MRI revealed other CSF exit routes especially around cranial nerves, the cribriform plate and cervical lymph nodes (Figure 2E). These other exit routes could explain the lack of accumulation of DOTA-Gd in the basal cisterna of anesthetized mice.

We also investigated whether there is a dose-response effect of isoflurane anesthesia on the accumulation of intracisternally administered DOTA-Gd. The surgical procedure was performed using 2.0-2.5% isoflurane to ensure sufficient anesthesia and then, the mice were switched to high-dose isoflurane (3.0%), low-dose isoflurane (1.5%) or allowed to recover (Figure 3A). 60 min thereafter, we assessed the brain distribution of DOTA-Gd by MRI. Our results revealed a dose-response effect of isoflurane anesthesia (Figure 3B-C). Whereas the use of 3% isoflurane significantly reduced the accumulation of DOTA-Gd in all brain regions compared to awake mice, the effect of 1.5% isoflurane was milder and significant in the cerebellum and olfactory bulbs only.

We then wanted to confirm the reduced diffusion of intracisternally administered DOTA-Gd in the brain parenchyma during general anesthesia using another anesthetic regimen. To this aim, we performed a similar experiment using ketamine/xylazine (100 mg/kg and 10 mg/kg, respectively) instead of isoflurane, since it was the anesthetic regimen that was used in the study by Xie *et al.* to demonstrate a higher activity of the glymphatic system during general anesthesia [15] (Figure 4A). In line with the results obtained using isoflurane, we observed a reduced parenchymal diffusion of DOTA-Gd in the brain of ketamine/xylazine anesthetized mice compared to awake mice as assessed by MRI 60 min after intracisternal injection (Figure 4B-C). This effect was consistent across all brain regions, except in the motor cortex where it did not reach statistical significance.

General anesthesia reduces the diffusion of intracisternally administered fluorescent dyes in the brain parenchyma.

In order to confirm those results using another imaging method, we performed both bright field photography and near infrared fluorescence (NIRF) imaging of the brain (*ex vivo*) 30 min after intracisternal injection of Evans Blue (Figure 5A). Macroscopically, Evans Blue distributed in the basal cisterna and surrounded the polygon of Willis in all animals, independently of the anesthetic regimen (Figure 5B). Interestingly, the hypothalamus surface was consistently stained in awake animals but remained free from Evans Blue in anesthetized animals. This discrepancy was in favor of an impaired distribution of Evans Blue in the brain of anesthetized mice. NIRF imaging further confirmed these results: intracisternal injection of Evans Blue was associated with rapid distribution of the fluorescent dye to the whole brain in awake animals (Figure 5C-D). In contrast, Evans Blue injected in the CSF of isoflurane-anesthetized mice showed a restricted distribution, limited to the basal cisterns of the brain, when compared with the awake group. Interestingly, the same results were obtained when using an anesthetic agent (ketamine) with a different mechanism of action (Figure 5A-D).

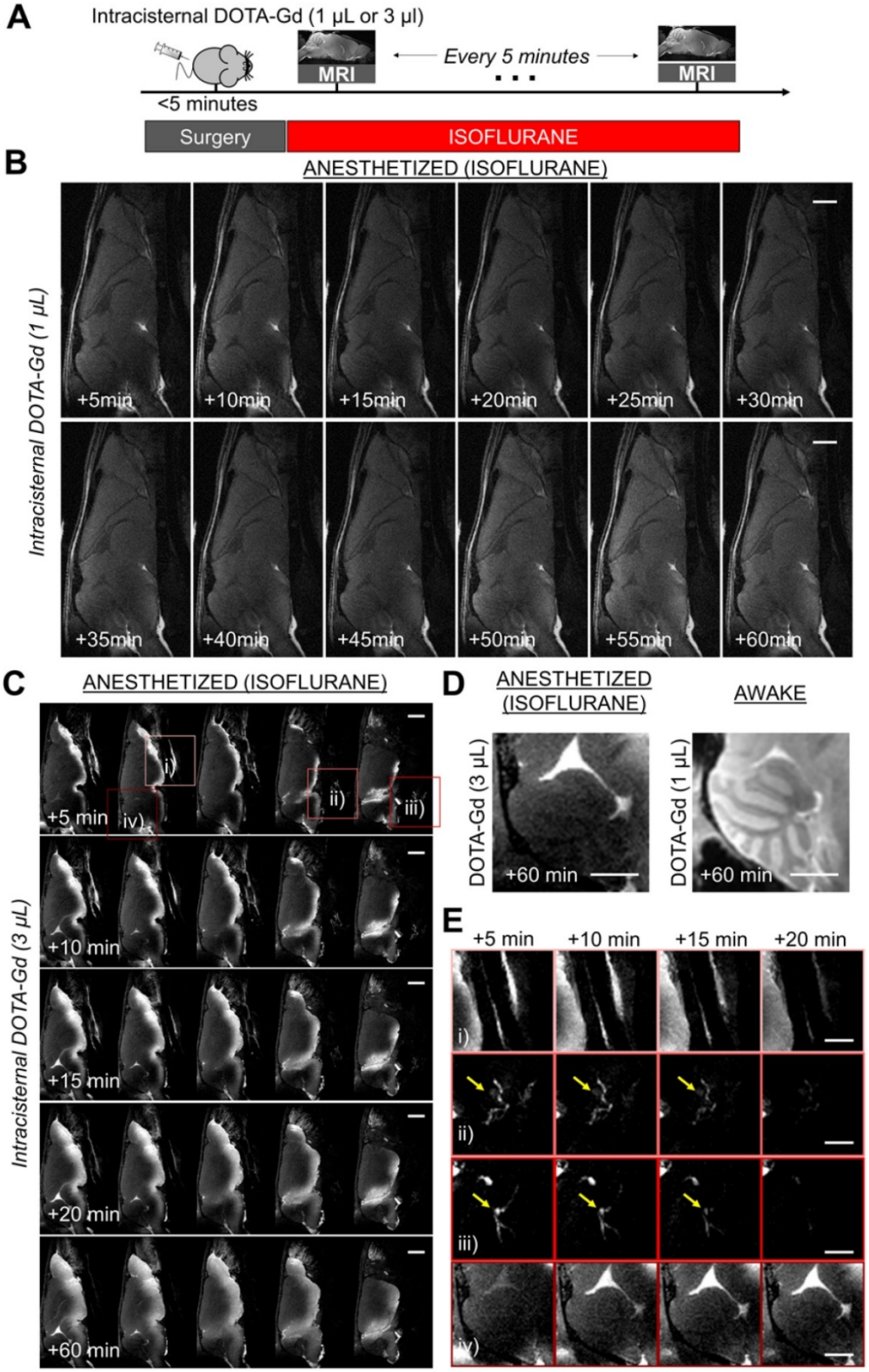

Figure 2. Longitudinal magnetic resonance imaging of the brain after intracisternal DOTA-Gd injection in isoflurane anesthetized mice. (A) Schematic representation of the experimental design of the longitudinal MRI experiments. **(B)** Representative MRI after intracisternal injection of 1 µL of DOTA-Gd in an anesthetized mouse (isoflurane 2-2.5%), showing only slight changes of MRI signal in the brain parenchyma of anesthetized mice in the first 60 min after injection. **(C)** Representative MRI after intracisternal injection of 3 µL of DOTA-Gd in an anesthetized mouse showing passive diffusion of DOTA-Gd inside the ventral part of the brain parenchyma. Note that the cerebellum remained free from DOTA-Gd even at the latest time point (+60 min). **(D)** Representative images of the cerebellum 60 min after DOTA-Gd administration in an anesthetized and an awake mouse (to allow direct comparison of the two experimental conditions). **(E)** Magnification of regions of interest from (C) corresponding to: i) airways, ii) cervical lymphatic vessels, iii) deep cervical lymph nodes (yellow arrows) and iv) cerebellum. These data demonstrate that the CSF is rapidly excreted from the brain by cervical lymphatic vessels in anesthetized mice. The cerebellum was chosen here because passive diffusion of DOTA-Gd does not occur in this region. Scale bar: 2 mm.

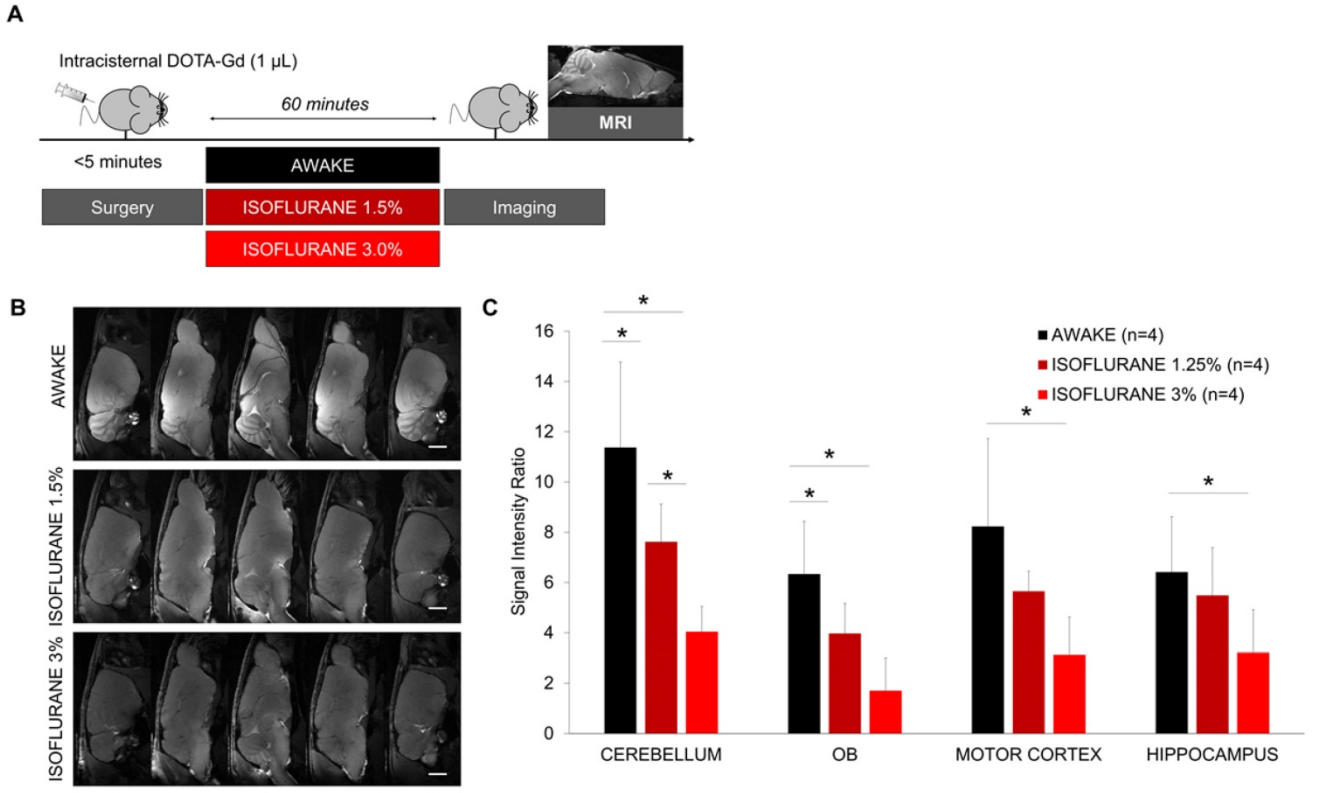

Figure 3. Dose-response effect of isoflurane on brain diffusion of intracisternally administered DOTA-Gd. (A) Schematic representation of the experimental design of the Magnetic Resonance Imaging (MRI) experiments. **(B)** Representative high-resolution T1-weighted images 60 min after intracisternal injection of DOTA-Gd (1 µL) in awake and anesthetized mice. **(C)** Corresponding quantification of the signal intensity in four different regions of interest (Cerebellum, Olfactory Bulbs (OB), Motor Cortex and Hippocampus). (n=4 mice per group). Scale bar: 2 mm.

Since sequential MRI during 60 consecutive minutes was not technically feasible in awake mice, we were not able to perform longitudinal and direct comparison of the distribution of intracisternally delivered DOTA-Gd between awake and anesthetized mice. To overcome this limitation, we developed an alternative method that takes advantage of a photomultiplier to dramatically increase the signal to noise ratio of NIRF images (Figure 6A-B). Using this method, the NIRF acquisition time was reduced to 22 ms, therefore, allowing real time *in vivo* NIRF imaging of freely moving mice (45 frames per second). We injected indocyanine green (which has a farther emission spectrum than Evans blue allowing deeper and more sensitive imaging) in the cisterna magna and performed longitudinal *in vivo* NIRF imaging of mice randomized to awake or anesthetized (isoflurane) state. Comparison of signal intensity between the two groups revealed that as soon as 30 min after intracisternal indocyanine green injection, there was significantly more indocyanine green in the forebrain of awake mice (Figure 6C-D and supplementary videos 1 and 2 showing that in anesthetized mice the tracer remains in the cisterna magna, whereas it diffuses in the forebrain of awake mice). These *in vivo* data further support that the intracranial circulation of CSF is more active in awake mice than in anesthetized mice.

General anesthesia does not significantly impact the brain interstitial space volume.

One study reported that the glymphatic activity is modulated by modification of the brain interstitial space [15]. Therefore, expansion of the brain interstitial space during sleep is associated with an increase in glymphatic activity [15]. In this previous study, the brain interstitial space was measured using ionotophoresis, an invasive method consisting of the measurement of ionic diffusion in the extracellular space. Several biases may have influenced these results, including the existence of a monodirectional convective flow from the injection electrode to the measuring electrode during the awake state (such as the glymphatic flow) [20]. Here, we evaluated the brain interstitial space volume using diffusion-weighted imaging and computation of the apparent diffusion coefficient of water (ADC), a validated method to estimate interstitial space diffusion parameters [29]. We measured the ADC by MRI in different regions of the brain of mice either awake or under isoflurane anesthesia (Figure 7A). A delay of 15 min after switching the anesthesia regimen

was respected before imaging to allow potential changes in interstitial volume to occur (this 15 min delay corresponds to the time needed for the extracellular volume to change after general anesthesia in a previous study [15]).

Fast imaging using echo-planar MRI allowed us to compute most ADC maps despite spontaneous movements of the awake mice (Figure 7B). The comparison of ADC calculated in different cerebral regions of interest in awake or anesthetized mice showed no significant variation between these two states (Figure 7C). To improve the sensitivity of the method, we pooled the values of 15 (awake) and 30 measurements (anesthetized). Nevertheless, there was still no significant difference between the ADC measured in awake or anesthetized mice (Figure 7D-E). Although we cannot rule out some slight changes of the ADC between these two states, our data do not support the reported 60% increase of the interstitial space during anesthesia [15].

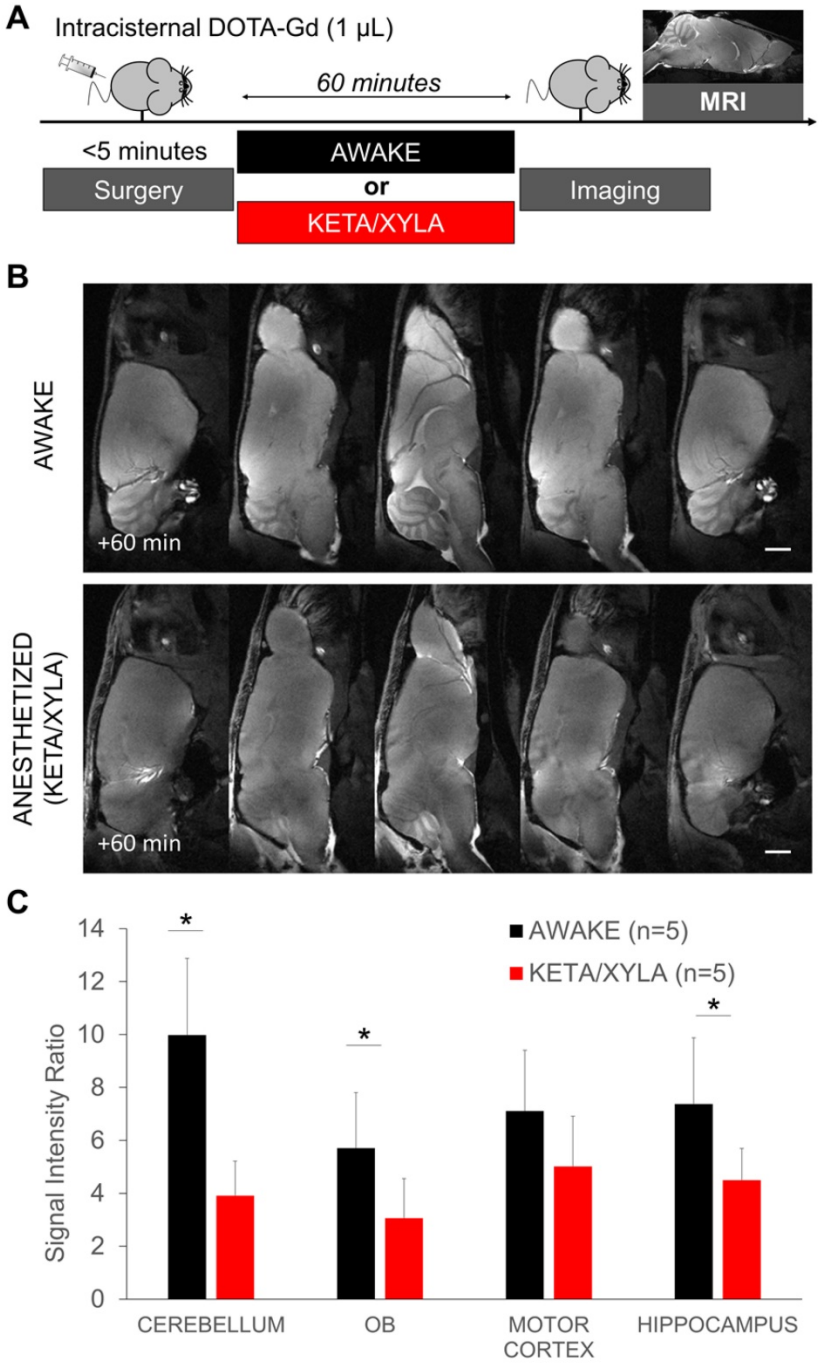

Figure 4. Gadolinium-enhanced magnetic resonance imaging after wakefulness or ketamine/xylazine general anesthesia. (A) Schematic representation of the experimental design of the Magnetic Resonance Imaging (MRI) experiments. **(B)** Representative high-resolution T1-weighted images 60 min after intracisternal injection of DOTA-Gd (1 µL) in awake (top) and anesthetized mice (bottom). **(C)** Corresponding quantification of the signal intensity in four different regions of interest (Cerebellum, Olfactory Bulbs (OB), Motor Cortex and Hippocampus). (n=5 mice per group). Scale bar: 2 mm.

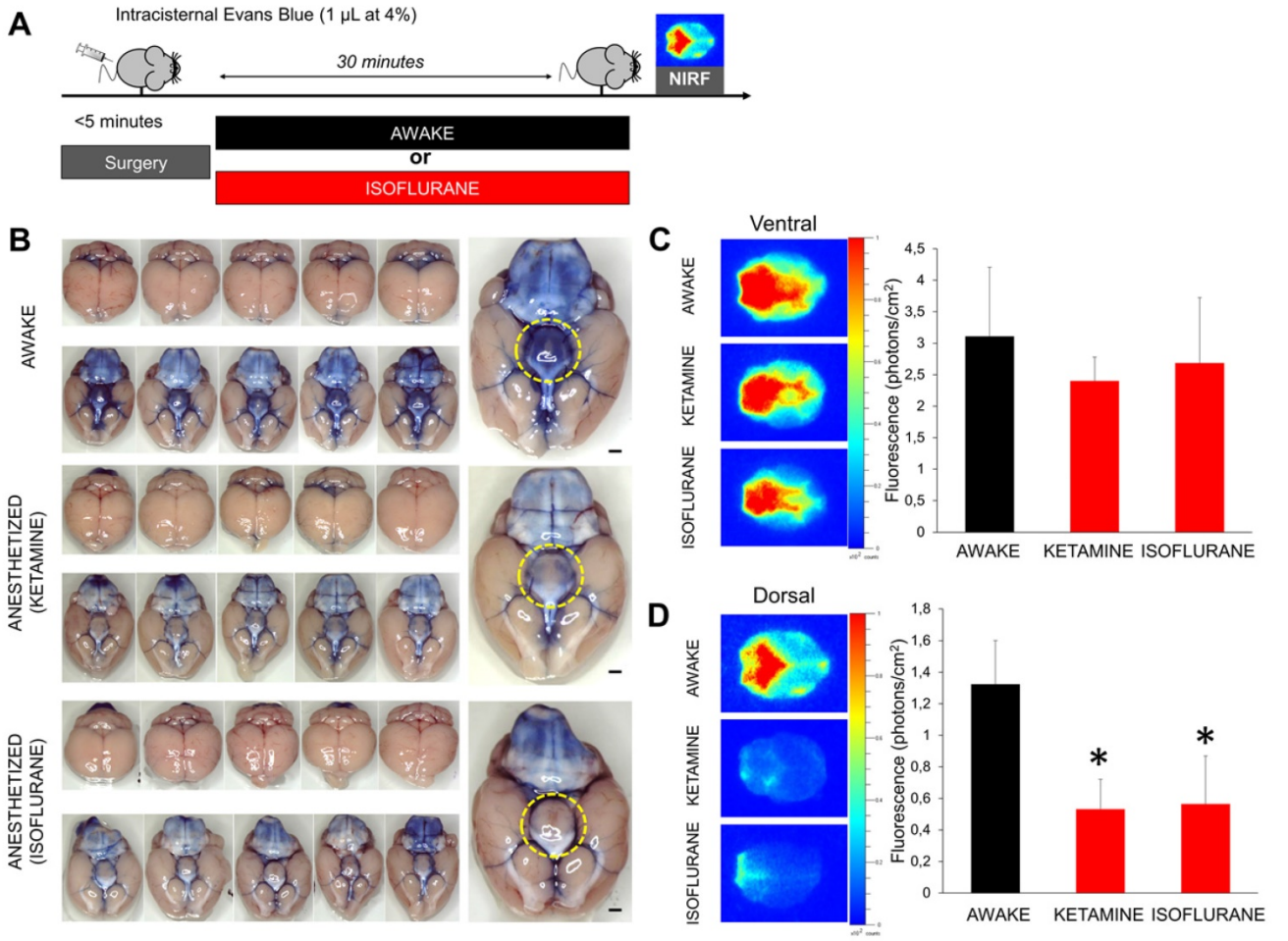

Figure 5. Evans blue enhanced near infrared fluorometry of the brain after wakefulness or general anesthesia. (A) Schematic representation of the experimental design of the near infrared fluorometry (NIRF) experiments. **(B)** Left: Bright field photographs of the ventral part of mouse brain 30 min after Evans Blue (1 µL at 4%) administration in the cisterna magna. Individual animals are represented. Right: Magnification of one representative animal per group. **(C)** Left: Representative *ex vivo* NIRF images (Excitation/Emission = 600/700 nm) of the ventral part of the brain (corresponding to the basal CSF cisterna) from animals in the awake and anesthetized (isoflurane 2% or ketamine 150 mg/kg) groups 30 min after Evans Blue administration in the cisterna magna. We can see that the fluorescent dye is distributed along the polygon of Willis in the perivascular spaces. Right: corresponding quantification showing no significant difference between the three experimental groups (n=5 mice/group). **(D)** Left: Representative *ex vivo* NIRF images of the dorsal part of the brain (corresponding to the brain parenchyma) from animals in the awake and anesthetized (isoflurane 2% or ketamine 150 mg/kg) groups 30 min after Evans Blue administration (1 µL at 4%) in the cisterna magna. The fluorescent dye is distributed in the cerebellum and along the large brain arteries (middle and anterior cerebral arteries) in the awake group. In contrast, almost no fluorescence was detectable in the two anesthetized groups of mice. Right: corresponding quantification showing significantly higher fluorescence intensity in the awake group (n=5 mice/group). These results demonstrate that diffusion of Evans blue in the brain parenchyma is significantly reduced by anesthesia. Scale bar: 2 mm.

Discussion

In the present study, we developed new methods to study CSF dynamics in the brain of anesthetized and awake mice. Altogether, our results demonstrate that i) CSF circulated through the brain during wakefulness, ii) the activity of this CSF circulation is reduced during general anesthesia and iii) the volume of the interstitial space does not significantly vary between the awake and anesthetized states in mice. These results are contradictory with the recent claims made by Nedergaard's group [15]. Although we confirm the existence of a CSF-mediated transport of low molecular weight compounds to the brain parenchyma [6], this flow of CSF is elevated in the awake state in comparison with the anesthetized state.

Methodological differences between our study and previous reports may explain the observed discrepancies [5]. We injected smaller volumes of tracer in the cisterna magna compared to previous studies on the glymphatic system (1 µL vs ~10 µL). Use of a large volume to infuse into the CSF of a mouse may have altered pressures and flows within the brain [7, 20]. Due to technical limitations, we were not able to measure the intracranial pressure during injection of the tracers in the CSF. A previous study from the literature imaging intracranial CSF circulation used an injection rate of 1.6 µL/min in the cisterna magna [30]. In another study, the intracranial pressure was not significantly increased 10 minutes after injection of 3 µl of a solution in the cisterna magna in mice [31]. In the present study, the injection rate was 1 µL/min except for the experiments presented in Figure 2 (3 µL/min). Even if we cannot exclude that different anesthetic regimens alter the

capacity of the brain parenchyma, CSF and vascular compartments to accommodate these volumes, these data suggest that the intracranial pressure was not significantly increased in experiments comparing awake to anesthetized animals. Moreover, we measured parenchymal influx of intracisternally administered contrast agents in the whole brain using MRI and NIRF, whereas the previous studies measured fluorescent dye influx in a restricted portion of the brain using two-photon microscopy [8, 15, 28]. In our study, the complete picture is in favor of an active parenchymal CSF circulation during wakefulness, which is reduced during general anesthesia, especially using high doses of isoflurane.

Still, there are major discrepancies in the observed diffusion of small molecule compounds injected in the CSF between studies that used MRI. In anesthetized rats, Iliff et al. failed to detect gadolinium in deep brain areas despite acquisitions performed up to 4 h after intracisternal injection, and observed enhancement in more superficial areas starting ~45 min after injection [28]. In serially imaged rats, Liu et al. observed a delayed diffusion of gadolinium chelate, which remained mostly within the CSF spaces, despite awake states between the successive scans [32]. In serially imaged mice, Petiet et al. observed that significant brain enhancement occurred more than 4 h after intraventricular injection of DOTA-Gd [33]. Differences in species, methods of gadolinium injection, anesthetic regimen and imaging procedure may explain those discrepancies. Moreover, the stress experienced by the mice after the surgical procedure might be a confounding factor in our experimental conditions. Therefore, other anesthetic agents, other anesthetic doses and the impact of general anesthesia in other species on the parenchymal diffusion of small molecular weight compounds deserve further investigation. Our dose response experiments suggest that the lower the dose of anesthetic agents, the smaller are their effects on CSF circulation, which may explain some discrepancies between the studies. Accordingly, we recently demonstrated that intracisternally administered DOTA-Gd rapidly diffuses in the brain parenchyma in non-human primates that were anesthetized using a low, clinical dose of propofol (0.05–0.25 mg/kg/min) [34]. According to our results, it is tempting to speculate that this diffusion would be even faster in awake animals.

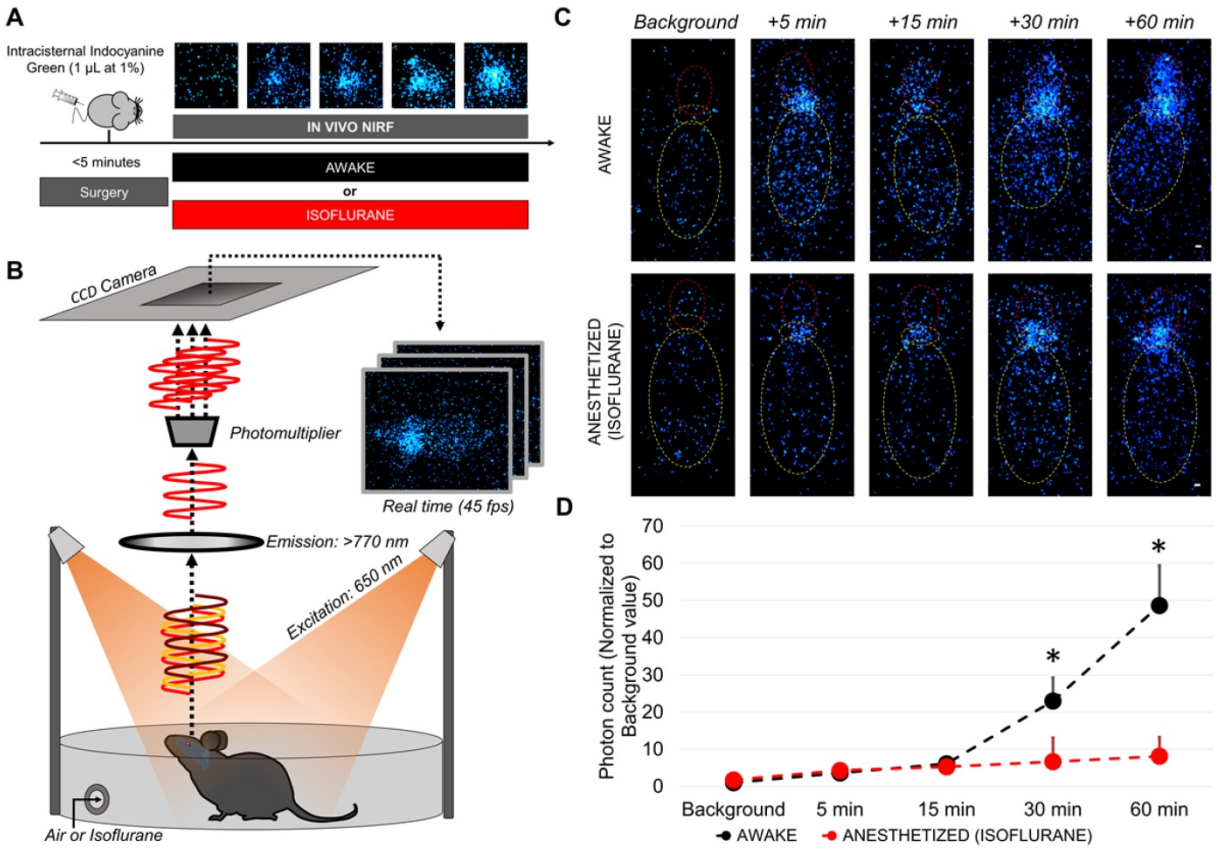

Figure 6. Longitudinal in vivo NIRF imaging of awake and anesthetized mice after intracisternal indocyanine green injection. (A) Schematic representation of the experimental design of the diffusion-weighted imaging experiments. **(B)** Schematic representation of the experimental setup for in vivo NIRF imaging of freely moving mice. **(C)** Representative *in vivo* NIRF images of an awake (top) and an anesthetized mice (bottom). Yellow: mouse body, orange: cisterna magna (indocyanine green injection site), red: forebrain. Whereas in awake mice the fluorescent tracer diffuses through the brain and is readily detectable in the forebrain, it remains near the injection site in the anesthetized mice. **(D)** Quantification of the data presented in (C) (n=4/group). * means significant vs anesthetized mice at the same time point. Scale bar: 2 mm.

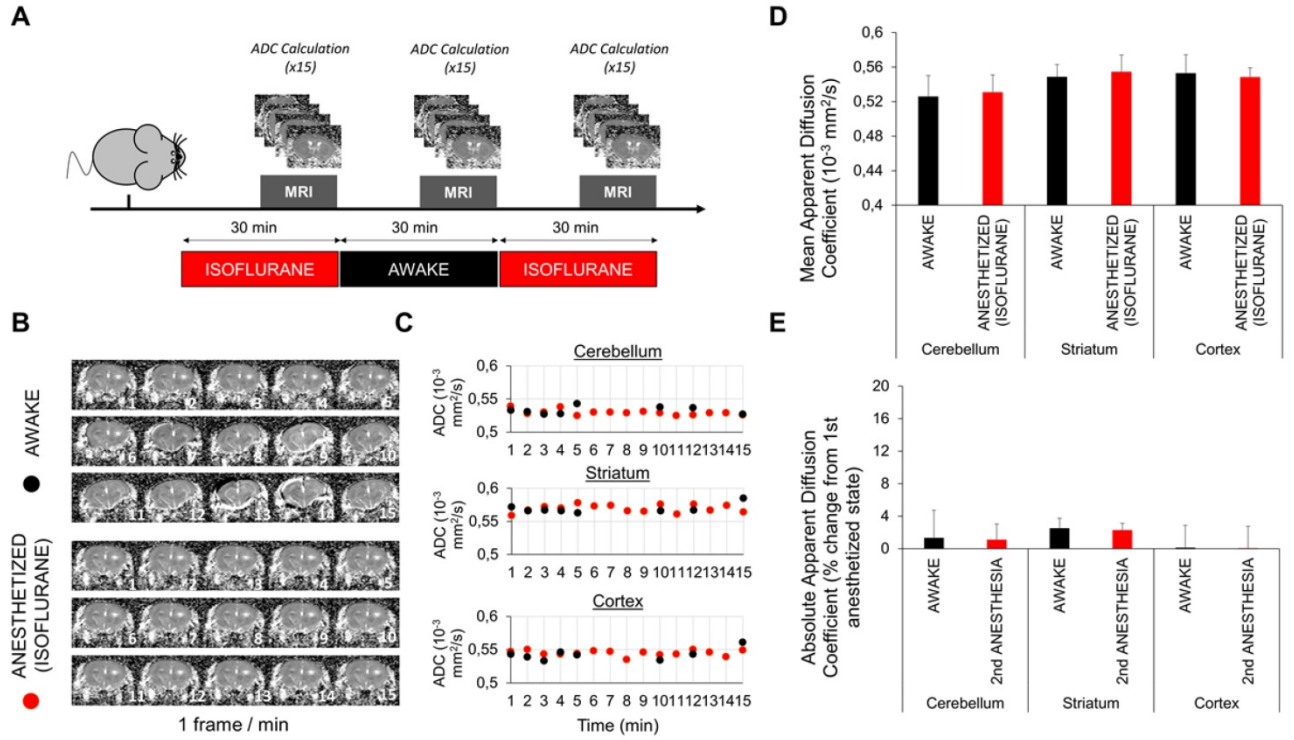

Figure 7. Diffusion-weighted magnetic resonance imaging in awake and anesthetized mice. (A) Schematic representation of the experimental design of the diffusion-weighted imaging experiments. We used 2.0-2.5% isoflurane in these experiments. **(B)** Representative Apparent Diffusion Coefficient (ADC) maps obtained in awake and anesthetized mice (1 frame per minute). Some movement is perceptible in awake but not in anesthetized mice. **(C)** ADC values in different brain regions of awake and anesthetized mice. Some points are missing in the awake group because the ADC maps of some timepoints were discarded because of movements. No difference is apparent. **(D)** Mean ADC values after pooling of the 15 (awake) and 30 measurements (anesthetized) in different parts of the brain (n=5). No significant difference was detected. **(E)** Absolute variation in percent of the ADC during awake and anesthetized states compared to the initial measurement of the ADC during the first period of anesthesia (n=5). No significant variation was found between experimental groups, arguing against change in the interstitial volume between general anesthesia and wakefulness.

Given the interactions between anesthesia and CSF circulation, the results of recent studies on the glymphatic system performed in anesthetized animals should be interpreted with caution. For instance, anesthesia may be a confounding factor in the studies regarding the diminished activity of the glymphatic system during aging or in animals with neurodegenerative disorders, since both conditions are associated with changes in anesthesia sensibility [35, 36]. New studies should therefore involve awake animals. Due to technical limitations, we were not able to perform the experiments in sleeping mice. Although the effects of naturally occurring sleep and general anesthesia on the glymphatic system were deemed to be equivalent [15], extrapolation of our findings from anesthesia to sleep should be done with caution. Another limitation of our study is the use of a short period of anesthesia to allow the intracisternal injection of contrast agents. This method was chosen because it is more reliable than catheter implantation to inject a small and reproducible volume, therefore avoiding the increase in brain intracranial pressure associated with large volume infusion while preserving the possibility to perform inter-animal comparison [20]. Moreover, the anesthesia time was reduced to a minimum of 5 min to limit its impact on the glymphatic system. In this regard, the pharmacokinetic and pharmacodynamic properties of volatile agents such as isoflurane allow rapid recovery from general anesthesia [37] (see also Figure S3, showing that the locomotor activity of mice after a 5 min period of isoflurane anesthesia is similar to non-anesthetized mice). Regarding NIRF imaging, it is important to consider that we used fluorescence intensity as a proxy for parenchymal distribution of the fluorescent tracer. Since NIRF imaging can detect fluorescence coming from several millimeters below the cortical surface, both the superficial tracer accumulation (in subarachnoid spaces) and intraparenchymal tracer accumulation were detected. Therefore, the observed differences can be explained both by a reduced surface coverage due to a slower CSF circulation and by a slower diffusion in the brain parenchyma. It should also be acknowledged that due to the relatively low spatial resolutions of the methods performed, we did not directly image paravascular influx of the paramagnetic and fluorescent tracers. It is possible that brain wide influx does not perfectly mirror perivascular influx.

The mechanisms driving the negative impact of

general anesthesia on the diffusion of DOTA-Gd in the brain parenchyma remain elusive, especially considering the contradictious reports published so far. Notably, most recent studies failed to support the existence of a convective flow of CSF in the brain parenchyma following a para-arterial entry route and a para-venular efflux [21-23] and thus invalidate the main proposal of the glymphatic system hypothesis. Rather, the results are consistent with a convective or dispersive CSF flow in the para-arterial spaces followed by passive diffusion in the brain parenchyma. In fact, our results are consistent with a dispersive flow in the paravascular spaces driven by cardiac and respiratory motions [38] allowing the injected DOTA-Gd to mix with the CSF, before its parenchymal diffusion from paravascular spaces through the pial sheath. During general anesthesia, the observed reduction in heart rate, blood pressure, arterial pulsatility and respiratory rate (Figure S4) could all participate in the reduction of the dispersive flow in the paravascular space and, therefore, prevent DOTA-Gd to diffuse into the brain parenchyma. This is further supported by the relationship between the anesthetic dose and the brain uptake of intracisternally injected DOTA-Gd that we observed. Another factor explaining discrepancies regarding CSF dynamics between awake and anesthetized brain could be related to a decreased rate of CSF production [39].

In conclusion, we evidenced that the CSF circulation from the basal cisterna to the brain parenchyma is more active in awake than in anesthetized mice. This result challenges the current view of wakefulness as a cerebral waste accumulation phase ahead of a cleaning phase mediated by the glymphatic system during general anesthesia (or more commonly, sleep). Our study raises the intriguing possibility that anesthesia for brain-injured patients may negatively impact neurological outcome by hampering the brain waste clearance system [25, 40]. Interestingly, a recent study demonstrated that surgery with anesthesia is associated with ventricular enlargement as well as cognitive and functional decline [41], in line with our current finding linking general anesthesia with CSF flow impairment.

Abbreviations

ADC: apparent diffusion coefficient; CSF: cerebrospinal fluid; DOTA-Gd: gadoterate; FLASH: fast low angle shot; ICG: indocyanine green; OB: Olfactory bulbs; MRI: magnetic resonance imaging; NIRF: near infrared fluorescence; SD: standard deviation.

Supplementary Material

Supplementary figures.
http://www.thno.org/v08p0710s1.pdf
Supplementary video 1.
http://www.thno.org/v08p0710s2.mp4
Supplementary video 2.
http://www.thno.org/v08p0710s3.mp4

Acknowledgments

This work was supported by grants from Société Française d'Anesthésie et Réanimation and Fondation pour la Recherche Médicale (SPE20150331891).

Authors' contribution

C.G., T.G., S.G., J.B., C.D.P., A.Q., S.M.D.L. and M.G. performed the experimental work. C.G. and M.G. carried out the statistical analysis. C.G., D.V. and M.G. analyzed the data. C.G. and M.G. designed the study and wrote the manuscript. All authors participated in manuscript revision.

Competing Interests

The authors have declared that no competing interest exists.

References

1. Cserr HF. Physiology of the choroid plexus. Physiol Rev. 1971; 51: 273-311.
2. Cserr HF, Cooper DN, Suri PK, Patlak CS. Efflux of radiolabeled polyethylene glycols and albumin from rat brain. Am J Physiol. 1981; 240: F319-28.
3. Cserr HF, Harling-Berg CJ, Knopf PM. Drainage of brain extracellular fluid into blood and deep cervical lymph and its immunological significance. Brain Pathol. 1992; 2: 269-76.
4. Carare RO, Bernardes-Silva M, Newman TA, Page AM, Nicoll JA, Perry VH, et al. Solutes, but not cells, drain from the brain parenchyma along basement membranes of capillaries and arteries: significance for cerebral amyloid angiopathy and neuroimmunology. Neuropathol Appl Neurobiol. 2008; 34: 131-44.
5. Brinker T, Stopa E, Morrison J, Klinge P. A new look at cerebrospinal fluid circulation. Fluids and barriers of the CNS. 2014; 11: 10.
6. Bedussi B, van der Wel NN, de Vos J, van Veen H, Siebes M, VanBavel E, et al. Paravascular channels, cisterns, and the subarachnoid space in the rat brain: A single compartment with preferential pathways. J Cereb Blood Flow Metab. 2016.
7. Bakker EN, Bacskai BJ, Arbel-Ornath M, Aldea R, Bedussi B, Morris AW, et al. Lymphatic Clearance of the Brain: Perivascular, Paravascular and Significance for Neurodegenerative Diseases. Cell Mol Neurobiol. 2016; 36: 181-94.
8. Iliff JJ, Wang M, Liao Y, Plogg BA, Peng W, Gundersen GA, et al. A paravascular pathway facilitates CSF flow through the brain parenchyma and the clearance of interstitial solutes, including amyloid beta. Sci Transl Med. 2012; 4: 147ra11.
9. Nedergaard M. Neuroscience. Garbage truck of the brain. Science. 2013; 340: 1529-30.
10. Strittmatter WJ. Bathing the brain. The Journal of clinical investigation. 2013; 123: 1013-5.
11. Tarasoff-Conway JM, Carare RO, Osorio RS, Glodzik L, Butler T, Fieremans E, et al. Clearance systems in the brain-implications for Alzheimer disease. Nat Rev Neurol. 2015; 11: 457-70.
12. Zeppenfeld DM, Simon M, Haswell JD, D'Abreo D, Murchison C, Quinn JF, et al. Association of Perivascular Localization of Aquaporin-4 With Cognition and Alzheimer Disease in Aging Brains. JAMA neurology. 2017; 74: 91-9.
13. Louveau A, Smirnov I, Keyes TJ, Eccles JD, Rouhani SJ, Peske JD, et al. Structural and functional features of central nervous system lymphatic vessels. Nature. 2015.
14. Aspelund A, Antila S, Proulx ST, Karlsen TV, Karaman S, Detmar M, et al. A dural lymphatic vascular system that drains brain interstitial fluid and macromolecules. The Journal of experimental medicine. 2015.
15. Xie L, Kang H, Xu Q, Chen MJ, Liao Y, Thiyagarajan M, et al. Sleep drives metabolite clearance from the adult brain. Science (New York, NY). 2013; 342: 373-7.

16. Xie Z, Dong Y, Maeda U, Moir RD, Xia W, Culley DJ, et al. The inhalation anesthetic isoflurane induces a vicious cycle of apoptosis and amyloid beta-protein accumulation. J Neurosci. 2007; 27: 1247-54.
17. Tang JX, Baranov D, Hammond M, Shaw LM, Eckenhoff MF, Eckenhoff RG. Human Alzheimer and inflammation biomarkers after anesthesia and surgery. Anesthesiology. 2011; 115: 727-32.
18. Palotas A, Reis HJ, Bogats G, Babik B, Racsmany M, Engvau L, et al. Coronary artery bypass surgery provokes Alzheimer's disease-like changes in the cerebrospinal fluid. J Alzheimers Dis. 2010; 21: 1153-64.
19. Groothuis DR, Vavra MW, Schlageter KE, Kang EW, Itskovich AC, Hertzler S, et al. Efflux of drugs and solutes from brain: the interactive roles of diffusional transcapillary transport, bulk flow and capillary transporters. J Cereb Blood Flow Metab. 2007; 27: 43-56.
20. Hladky SB, Barrand MA. Mechanisms of fluid movement into, through and out of the brain: evaluation of the evidence. Fluids and barriers of the CNS. 2014; 11: 26.
21. Smith AJ, Yao X, Dix JA, Jin BJ, Verkman AS. Test of the 'glymphatic' hypothesis demonstrates diffusive and aquaporin-4-independent solute transport in rodent brain parenchyma. eLife. 2017; 6.
22. Asgari M, de Zelicourt D, Kurtcuoglu V. Glymphatic solute transport does not require bulk flow. Sci Rep. 2016; 6: 38635.
23. Jin BJ, Smith AJ, Verkman AS. Spatial model of convective solute transport in brain extracellular space does not support a "glymphatic" mechanism. J Gen Physiol. 2016; 148: 489-501.
24. Lee H, Xie L, Yu M, Kang H, Feng T, Deane R, et al. The Effect of Body Posture on Brain Glymphatic Transport. J Neurosci. 2015; 35: 11034-44.
25. Gaberel T, Gakuba C, Goulay R, Martinez De Lizarrondo S, Hanouz JL, Emery E, et al. Impaired glymphatic perfusion after strokes revealed by contrast-enhanced MRI: a new target for fibrinolysis? Stroke. 2014; 45: 3092-6.
26. Belliere J, Martinez de Lizarrondo S, Choudhury RP, Quenault A, Le Behot A, Delage C, et al. Unmasking Silent Endothelial Activation in the Cardiovascular System Using Molecular Magnetic Resonance Imaging. Theranostics. 2015; 5: 1187-202.
27. Briens A, Gauberti M, Parcq J, Montaner J, Vivien D, Martinez de Lizarrondo S. Nano-zymography Using Laser-Scanning Confocal Microscopy Unmasks Proteolytic Activity of Cell-Derived Microparticles. Theranostics. 2016; 6: 610-26.
28. Iliff JJ, Lee H, Yu M, Feng T, Logan J, Nedergaard M, et al. Brain-wide pathway for waste clearance captured by contrast-enhanced MRI. The Journal of clinical investigation. 2013; 123: 1299-309.
29. Vorisek I, Sykova E. Measuring diffusion parameters in the brain: comparing the real-time iontophoretic method and diffusion-weighted magnetic resonance. Acta physiologica. 2009; 195: 101-10.
30. Yang L, Kress BT, Weber HJ, Thiyagarajan M, Wang B, Deane R, et al. Evaluating glymphatic pathway function utilizing clinically relevant intrathecal infusion of CSF tracer. J Transl Med. 2013; 11: 107.
31. Mathieu E, Gupta N, Macdonald RL, Ai J, Yucel YH. In vivo imaging of lymphatic drainage of cerebrospinal fluid in mouse. Fluids and barriers of the CNS. 2013; 10: 35.
32. Liu CH, D'Arceuil HE, de Crespigny AJ. Direct CSF injection of MnCl(2) for dynamic manganese-enhanced MRI. Magn Reson Med. 2004; 51: 978-87.
33. Petiet A, Santin M, Bertrand A, Wiggins CJ, Petit F, Houitte D, et al. Gadolinium-staining reveals amyloid plaques in the brain of Alzheimer's transgenic mice. Neurobiol Aging. 2012; 33: 1533-44.
34. Goulay R, Flament J, Gauberti M, Naveau M, Pasquet N, Gakuba C, et al. Subarachnoid Hemorrhage Severely Impairs Brain Parenchymal Cerebrospinal Fluid Circulation in Nonhuman Primate. Stroke. 2017; 48: 2301-5.
35. Kanonidou Z, Karystianou G. Anesthesia for the elderly. Hippokratia. 2007; 11: 175-7.
36. Kress BT, Iliff JJ, Xia M, Wang M, Wei HS, Zeppenfeld D, et al. Impairment of paravascular clearance pathways in the aging brain. Ann Neurol. 2014; 76: 845-61.
37. Gupta A, Stierer T, Zuckerman R, Sakima N, Parker SD, Fleisher LA. Comparison of recovery profile after ambulatory anesthesia with propofol, isoflurane, sevoflurane and desflurane: a systematic review. Anesth Analg. 2004; 98: 632-41.
38. Yamada S, Miyazaki M, Yamashita Y, Ouyang C, Yui M, Nakahashi M, et al. Influence of respiration on cerebrospinal fluid movement using magnetic resonance spin labeling. Fluids and barriers of the CNS. 2013; 10: 36.
39. Artru AA. Effects of halothane and fentanyl on the rate of CSF production in dogs. Anesthesia and analgesia. 1983; 62: 581-5.
40. Brinjikji W, Murad MH, Rabinstein AA, Cloft HJ, Lanzino G, Kallmes DF. Conscious sedation versus general anesthesia during endovascular acute ischemic stroke treatment: a systematic review and meta-analysis. AJNR Am J Neuroradiol. 2015; 36: 525-9.
41. Schenning KJ, Murchison CF, Mattek NC, Silbert LC, Kaye JA, Quinn JF. Surgery is associated with ventricular enlargement as well as cognitive and functional decline. Alzheimer's & dementia : the journal of the Alzheimer's Association. 2016; 12: 590-7.